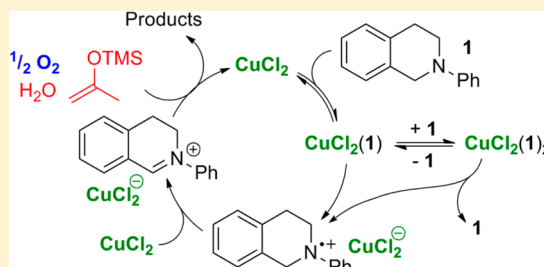


Reaction Progress Kinetic Analysis of a Copper-Catalyzed Aerobic Oxidative Coupling Reaction with *N*-Phenyl TetrahydroisoquinolineMartin Scott,[‡] Abhishek Sud,[†] Esther Boess,[†] and Martin Klussmann^{*,†}[†]Max-Planck-Institut fuer Kohlenforschung, Kaiser-Wilhelm-Platz 1, 45470 Muelheim an der Ruhr, Germany[‡]Department of Chemistry, Cologne University, Greinstrasse 4, 50939 Koeln, Germany

S Supporting Information

ABSTRACT: The results from a kinetic investigation of a Cu-catalyzed oxidative coupling reaction between *N*-phenyl tetrahydroisoquinoline and a silyl enol ether using elemental oxygen as oxidant are presented. By using reaction progress kinetic analysis as an evaluation method for the obtained data, we discovered information regarding the reaction order of the substrates and catalysts. Based on this information and some additional experiments, a refined model for the initial oxidative activation of the amine substrate and the activation of the nucleophile by the catalyst was developed. The mechanistic information also helped to understand why silyl nucleophiles have previously failed in a related Cu-catalyzed reaction using *tert*-butyl hydroperoxide as oxidant and how to overcome this limitation.

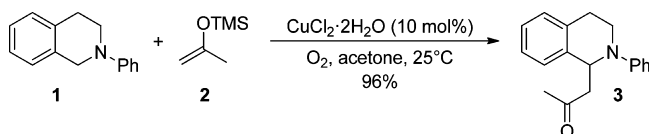


INTRODUCTION

Oxidative coupling reactions, also called cross-dehydrogenative coupling (CDC) reactions, have received considerable interest in recent years due to their ability to directly convert two C–H bonds into a new C–C bond.¹ Such a transformation makes prior activation or introduction of leaving groups unnecessary and thus can help to streamline synthesis, save time and materials, and reduce the amount of waste, thereby contributing to sustainable chemistry. The use of air or oxygen as oxidant is very attractive as an abundant and low-cost reagent that also creates at best only water as the waste product.² Among the many substrates that can be utilized in such reactions, amines and most notably *N*-aryl tetrahydroisoquinolines stand out because they have seen the development of a large number of methods for their oxidative coupling with other substrates, mostly reactive nucleophiles.^{3,4} However, more detailed investigations of the mechanism of these reactions have only recently begun, and some issues remain unsolved.⁵

Previously, we reported experimental mechanistic studies of the oxidative coupling reaction between *N*-phenyl tetrahydroisoquinoline (**1**) and various nucleophiles, including silyl enol ether **2**, catalyzed by copper(II) chloride dihydrate under an oxygen atmosphere (Scheme 1).⁶

Scheme 1. Oxidative Coupling Reaction under Study in This Investigation



This reaction was originally developed by our group in order to introduce carbonyl residues into the α -position of *N*-aryl amines, giving products like **3**.⁷ With *N*-aryl tetrahydroisoquinolines, generally clean reactions with high yields are achieved, which make these reactions very suitable for mechanistic studies. We could characterize and isolate the reactive intermediate of this reaction, iminium dichlorocuprate **4**, which is formed upon reaction with Cu(II), providing the coupling products after conversion with any nucleophile of sufficient reactivity (Scheme 2a).⁶ In the presence of water (the reactions are performed without prior purification of reagents and solvent) or methanol (the solvent of choice for nucleophiles of lower reactivity), an off-cycle equilibrium is established between iminium **4** and a hemiaminal (R = H) or hemiaminal ether (R = Me) **5**. These species can be beneficial for the final product yield if less reactive nucleophiles are utilized, as they provide a reservoir for the reactive iminium ion **4**, which otherwise can undergo undesired side reactions.

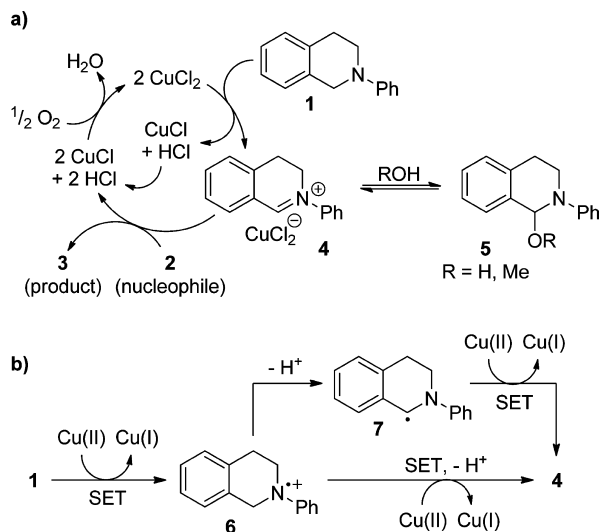
For the generation of iminium **4** from **1**, a combination of single electron transfer (SET) and proton transfer steps is usually suggested (Scheme 2b).^{5f,6b,8} After one SET step, for example, by reaction with the high valent Cu catalyst, an ammoniumyl radical cation **6** is formed. The iminium ion **4** presumably is formed either stepwise by deprotonation to give C-radical **7** and subsequent SET or directly by hydrogen atom transfer.^{5a,9} The latter scenario, proton-coupled electron transfer, has been suggested in a computational study by Cheng et al. for the Cu-catalyzed oxidative coupling with **1**.^{5b}

Special Issue: Mechanisms in Metal-Based Organic Chemistry

Received: August 15, 2014

Published: September 9, 2014

Scheme 2. (a) Previously Proposed Mechanism for the Reaction of Scheme 1 and (b) Proposed Formation of the Iminium Ion 4 from 1 by Single Electron Transfer and Proton Transfer Steps



We could previously show that $\text{CuCl}_2 \cdot 2\text{H}_2\text{O}$ alone can mediate this transformation and that oxygen is not required, suggesting that the SET steps involve $\text{Cu}(\text{II})$ directly and that the role of oxygen is to reoxidize the reduced catalyst.^{6b}

Herein, we report the results from kinetic studies of the reaction shown in Scheme 1 using reaction progress kinetic analysis¹⁰ as the method to evaluate the data. Silyl enol ether 2 was considered to be particularly suitable as it is one of the fastest reacting substrates in a series of C–H and silyl nucleophiles in previous investigations,⁶ which could facilitate the elucidation of kinetic details of the oxidation of amine 1. The reaction time scale of several minutes to a few hours and its exothermic nature make it very suitable for obtaining kinetic data by reaction calorimetry. This in situ technique delivers heat flow data, which are directly proportional to the reaction rate, over the entire course of the reaction. Thus, it is a method of choice for reaction progress kinetic analysis,¹¹ relying on a large kinetic data set with good quality for graphical data evaluation, which is discussed in the following.

RESULTS AND DISCUSSION

The reaction of Scheme 1 was performed in a reaction calorimeter at 25 °C, under essentially the same conditions as those reported previously for synthetic purpose.⁷ Parallel analysis of a reaction by reaction calorimetry and ^1H NMR (by taking several samples over the course of the reaction) revealed that the reaction profiles obtained by both methods were essentially identical. The heat flow data obtained from calorimetric experiments were converted to reaction rate and conversion profiles as described in the Experimental Section, following established procedures.^{10b} As a reference for further kinetic studies, a “standard reaction” was defined, using 0.012 M $\text{CuCl}_2 \cdot 2\text{H}_2\text{O}$ (10 mol %), 0.12 M amine 1, and 0.19 M enol ether 2 in acetone at 25 °C (Figure 1). The curves derived from repeated experiments were found to be reproducible within an acceptable scope of deviation (see the Supporting Information).

Same Excess Experiment. In order to probe for potential problems like catalyst deactivation, a “same excess” experiment was performed, which effectively models the standard reaction

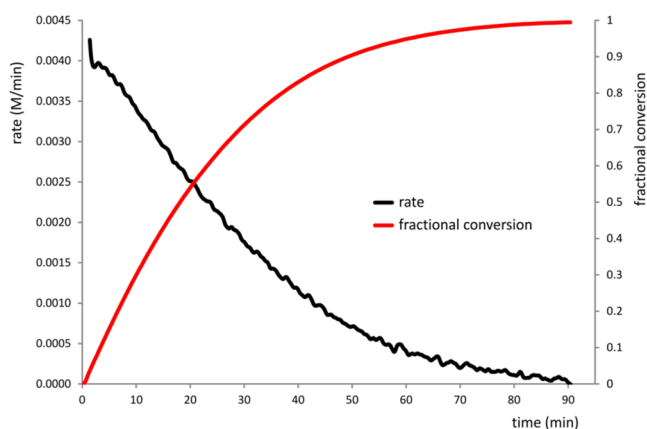


Figure 1. Reaction rate (black line) and conversion (red line) profiles of the standard reaction using 0.012 M $\text{CuCl}_2 \cdot 2\text{H}_2\text{O}$, 0.123 M 1, and 0.185 M 2 in acetone at 25 °C.

after a certain conversion. Herein, excess is defined as the concentration excess, [excess], of the enol ether 2 over the limiting reagent, amine 1 (eq 1).

$$[\text{excess}] = [\mathbf{2}] - [\mathbf{1}] \quad (1)$$

Figure 2 shows a plot of reaction rate versus the concentration of the amine substrate, also called a “graphical rate equation”.¹⁰

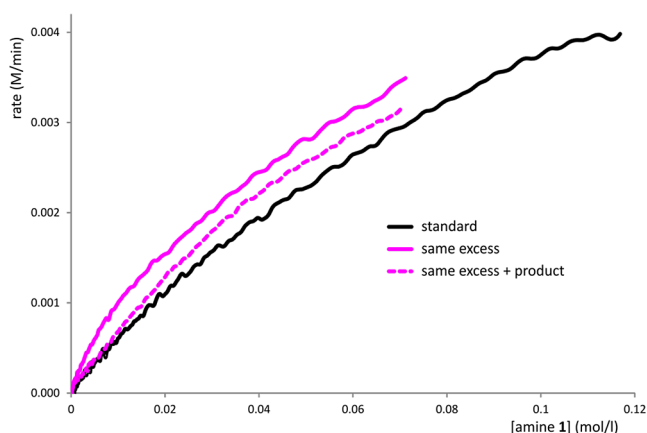


Figure 2. Same excess experiment and the effect of added product under standard conditions. Standard (black line): 0.123 M 1, 0.185 M 2. Same excess (magenta line): 0.081 M 1, 0.141 M 2. Same excess + product (magenta dashed line): 0.081 M 1, 0.143 M 2, 0.041 M 3. All experiments: 0.012 M $\text{CuCl}_2 \cdot 2\text{H}_2\text{O}$, acetone, 25 °C.

Note that the reaction progress is plotted from right to left. Clearly, it can be seen that the same excess experiment does not overlay with the experiment run under standard conditions but lies slightly above.

The same excess experiment starts with substrate concentrations as present in the standard reaction after approximately 34% conversion, without the product being present and without any turnover of the catalyst. The fact that the rate of the standard reaction is lower at each concentration of amine 1 could indicate catalyst deactivation. To probe for inhibition by the product, the same excess experiment was repeated in the presence of 0.04 M product—the amount that corresponds to approximately 34% conversion. As seen in Figure 2, this has some diminishing effect on the rate, although it still does not overlay with the standard reaction curve. Accordingly, some

degree of product inhibition occurs, but another effect is also slightly reducing the rate during the reaction progress. This could be the precipitation of insoluble $\text{CuCl}(\text{OH})$, formed from CuCl by oxidation in the presence of water, which has been characterized before in reactions at very high catalyst loading of 50 mol %.^{6a}

Catalyst Reaction Order. To determine the reaction order of the catalyst, five experiments with different catalyst concentrations ranging from 10 to 24 mol % of $\text{CuCl}_2 \cdot 2\text{H}_2\text{O}$ were conducted while keeping all other reaction parameters the same as in the standard reaction. The “graphical rate equation” plot shows a clear increase in rate upon increasing the initial catalyst concentration, indicating a positive reaction order (Figure 3a).

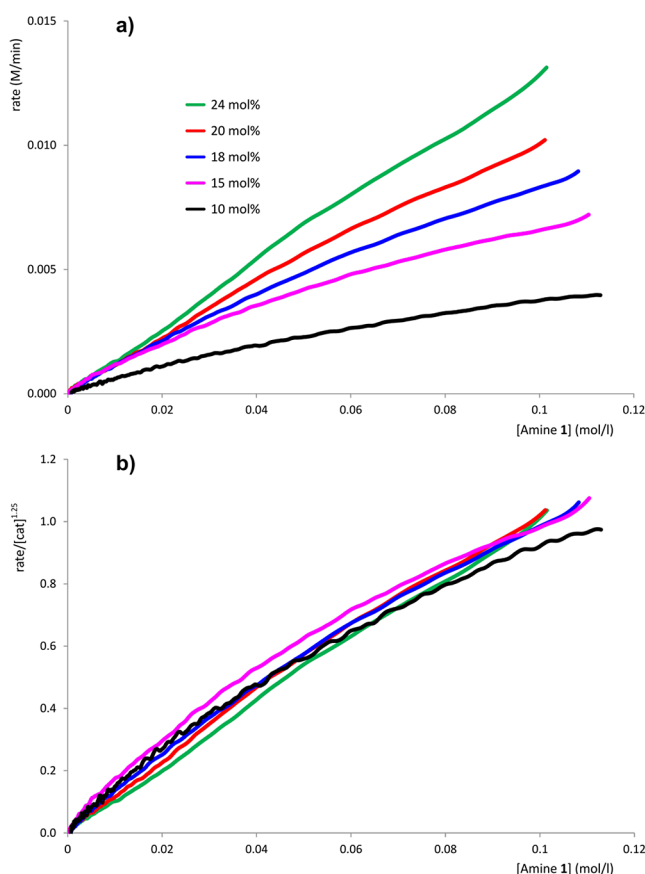


Figure 3. (a) Reaction rate versus amine concentration at different catalyst concentrations. (b) Reaction rate divided by initial catalyst concentration to the power of 1.25, achieving overlay of the different curves. $\text{CuCl}_2 \cdot 2\text{H}_2\text{O}$ concentrations: 10 mol % (standard, black line), 0.012 M; 15 mol % (magenta line), 0.018 M; 18 mol % (blue line), 0.022 M; 20 mol % (red line), 0.025 M; 24 mol % (green line), 0.030 M. All experiments: 0.12 M **1**, 0.18 M **2**, acetone, 25 °C.

The apparent reaction order of the catalyst, x , can be determined from this data set by dividing the reaction rate r by the initial concentration of the catalyst taken to the power of the reaction order.¹⁰ This should cause the curves from the experiments with different catalyst concentrations to overlay, given that their rates differ only by the factor of $[\text{catalyst}]^x$, and all other parameters are being kept constant. As depicted, this was found to be the case for a reaction order larger than 1 with a value of approximately 1.25 (Figure 3b). This value suggests a

complex reaction mechanism with a combination of steps involving more than one molecule of catalyst.

Since it was proposed that the oxidation of **1** is mediated by two molecules of $\text{Cu}(\text{II})$, as visualized in Scheme 2b, it is reasonable to assume that both SET steps are contributing to the reaction rate equation. A consecutive reaction of **1** with two molecules of CuCl_2 , first to form the radical cation **6** and then to form the iminium ion **4**, would result in a higher order rate dependence on $[\text{CuCl}_2]$. Alternatively, the apparent reaction order in the catalyst could be related to the reoxidation of $\text{Cu}(\text{I})$ to $\text{Cu}(\text{II})$ by oxygen. For example, the reoxidation of simple copper–amine complexes has been shown to involve four molecules of $\text{Cu}(\text{I})$.¹²

The graphical evaluation as shown in Figure 3a might not be precise enough to distinguish between true first order and higher order reactions, given the error range of the experiments and the fact that the graphical overlay is not perfect. Thus, the same set of data was used to derive the reaction order in the catalyst by plotting rates versus catalyst loading and fitting the data to linear or power law functions. This also indicated that values of around 1.25 are very likely, although a value of 1.0 could not be ruled out with certainty. The same apparent catalyst reaction order of 1.25 was also obtained from graphical rate equations when the experiments were conducted at lower excess of enol ether **2** (see the Supporting Information; also see below for a discussion of the effects of enol ether concentration). It has been shown before that this graphical evaluation of obtaining kinetic information is in reasonable agreement with mathematical approaches.^{10c}

Different Excess Experiment: Amine Reaction Order.

Different excess experiments¹⁰ were conducted to probe for the reaction order of the amine substrate, varying its concentration while keeping all other parameters at standard conditions. As can be seen from the plot of rate versus enol ether concentration, the reaction rate increases with decreasing [excess], that is, with increasing amine concentration (Figure 4a). Accordingly, the concentration of amine **1** has a positive influence on the reaction rate and is expected to have a positive reaction order. As for the experiment probing the catalyst's reaction order above, the reaction order for the amine can be determined from this data set by dividing the reaction rate r at any time by the concentration of **1** at that time, taken to the power of x . The best overlay was achieved in this case for a reaction order x of 0.45 (Figure 4b).

The fact that the curves in Figure 4b stop to overlay at higher conversions, that is, at lower enol ether concentrations, can be rationalized because the concentration of **1**, the limiting reagent, approaches zero at these stages. Under such conditions, the reaction rate necessarily approaches zero also and the data toward the end of the reaction are best excluded from the comparison of the rate curves.^{10b} Two possibilities of interpreting the amine reaction order of 0.45 come to mind. The reaction order could appear to be smaller than 1 because of saturation kinetics, due to strong binding between the copper catalyst and amine **1**. This would result in the reaction rate becoming independent of [amine] at high concentrations, and the resting state of the catalyst would be a Cu–amine complex. However, both cases could not be further investigated; at the highest possible amine concentration that we could investigate, the rate was still dependent on its concentration, and upon mixing $\text{CuCl}_2 \cdot 2\text{H}_2\text{O}$ with **1**, rapid oxidation to the iminium salt **4** occurs.⁶ A second explanation for a fractional reaction order could be the involvement of species containing two or more

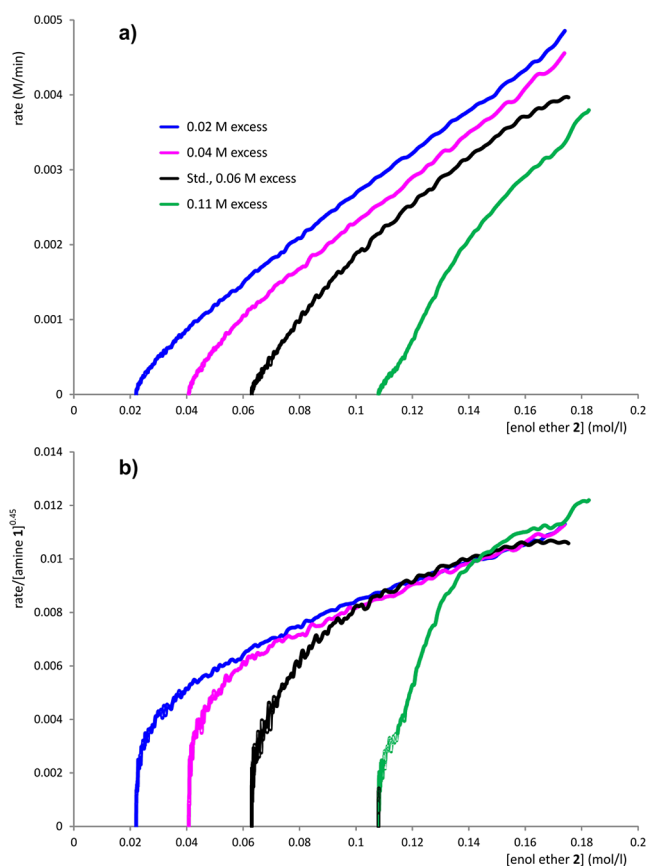
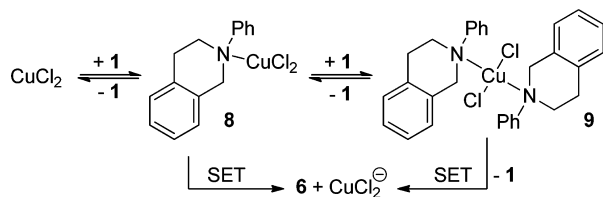


Figure 4. Different excess experiments varying the concentration of the amine **1**; (a) reaction rate versus enol ether (**2**) concentration; (b) reaction rate divided by $[1]$ to the power of 0.45, achieving overlay of the different curves. Concentrations of **1**: 0.11 M excess (green line), 0.080 M; Std., 0.06 M excess (black line), 0.123 M; 0.04 M excess (magenta line), 0.143 M; 0.02 M excess (blue line), 0.163 M. All experiments: 0.012 M $\text{CuCl}_2 \cdot 2\text{H}_2\text{O}$, 0.18 M **2**, acetone, 25 °C.

molecules of **1**. For example, a rapid equilibrium could exist between copper complexes **8** and **9** with one and two amines as the ligand, respectively (Scheme 3). Cu(II) is known to favor four-fold coordination, making the rapid formation of **9** in the presence of an excess of **1** likely.

Scheme 3. Potential Reason for the Fractional Amine Reaction Order, Equilibria between Copper Complexes **8 and **9** Containing One and Two Molecules of Amine **1** and Formation of Radical Cation **6** from **8** and **9**, Respectively, after Dissociation of **1****



The subsequent SET reaction could occur directly from complex **8**, from **9** after dissociation of one molecule of **1**, or from **9** directly by dissociation into the ammoniumyl radical cation **6** and amine **1**. In the computational study by Cheng et al., water was used as an auxiliary ligand on Cu(II) for the SET reaction of Scheme 2b;^{5b} this role could also be taken over by a

second molecule of **1**. The counterion of **6** is likely to be dichlorocuprate, in analogy to the iminium salt **4**.

In a series of related experiments at lower [excess], essentially the same result was obtained, that is, a reaction order of 0.45 for amine **1** (see the Supporting Information).

Different Excess Experiment: Silyl Enol Ether Reaction Order. To determine the reaction order for enol ether **2**, a new set of different excess experiments was conducted, this time varying the concentration of **2** while keeping all other parameters the same as in the standard experiment. The evaluation for the same excess experiment was performed as described above by variation of the amine concentrations. The plot of reaction rate versus [amine] shows that the rate increases slightly upon increasing the enol ether concentration up to 0.24 M (Figure 5a). When the enol ether concentration

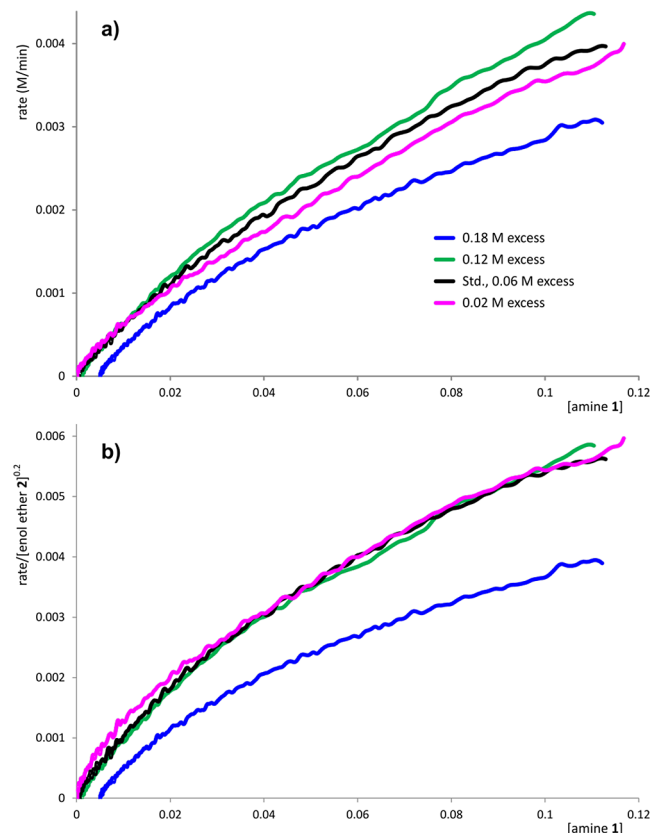


Figure 5. Different excess experiments varying the concentration of enol ether **2**; (a) reaction rate versus [amine]; (b) reaction rate divided by $[2]$ to the power of 0.2, achieving overlay of the different curves. Concentrations of **2**: 0.02 M excess (magenta line), 0.142 M; Std., 0.06 M excess (black line), 0.185 M; 0.12 M excess (green line), 0.241 M; 0.18 M excess (blue line), 0.302 M. All experiments: 0.012 M $\text{CuCl}_2 \cdot 2\text{H}_2\text{O}$, 0.12 M **1**, acetone, 25 °C.

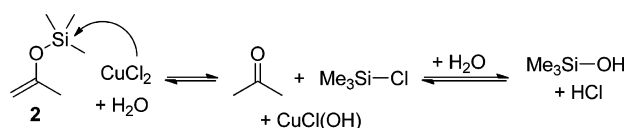
was further increased to 0.30 M (0.18 M excess), the rate drops below that of the experiment with the lowest concentration of **2** (0.02 M excess).

Good overlay was found by dividing the rate curves by $[\text{enol ether}]^{0.2}$, indicating an apparent reaction order in **2** of 0.2 (Figure 5b). As expected, an overlay is not achieved for the curve of the “0.18 M excess” experiment. The low reaction order found for enol ether concentrations up to 0.24 M (0.12 M excess) could indicate that the addition of nucleophile is partially rate-controlling but that a preceding step dominates

the rate equation, making the reaction order nearly zero for the enol ether. As the deviation between these rate curves is small and similar to the one seen in repetitive experiments of the standard experiment, it is supposable that it lies within the error of measurement and the reaction order in **2** is actually zero. This is in line with our previous studies, in which **2** was found to be one of the fastest reacting nucleophiles and the intermediates **4** and **5** were basically not visible during the reaction progress, in contrast to slower reacting nucleophiles.⁶

The drop in reaction rate seen for the “0.18 M excess experiment” indicates an unfavorable interaction dominating at high enol ether concentrations, being a reproducible observation. As there is no detectable interaction between substrates **1** and **2** in the absence of catalyst, it is reasonable to assume an interaction between **2** and the catalyst. The well-known reactivity of silyl groups toward halide nucleophiles, which is used in the activation of silyl nucleophiles as well as the deprotection of silyl protecting groups, comes to mind. A reaction between CuCl_2 and enol ether **2** could mediate O–Si bond cleavage by attack of a chloride ion on silicon, leading to a loss of chloride from the catalyst. The formed trimethylsilyl chloride will eventually be hydrolyzed, releasing the chloride (Scheme 4).

Scheme 4. Possible Interactions between Enol Ether **2, CuCl_2 Catalyst, and Water**



At high enol ether concentrations, this reaction could dominate over interactions between the catalyst and the amine, and the concentration of water in the system may no longer be high enough to ensure efficient hydrolysis of trimethylsilyl chloride. Thus, the formation of insoluble CuCl(OH) or other species of lower chloride content could reduce the catalyst's activity of the reaction. For example, the use of CuCl as catalyst in the reaction of Scheme 1 increased the reaction time and reduced the yield of **3**.⁷ In line with this rationale, adding water to the reaction at high enol ether concentration significantly increased its rate. This effect also occurs at lower enol ether concentrations; for example, conducting the standard reaction in the presence of 2.4 M water, full conversion is achieved after 15 instead of 100 min. Preliminary experiments with the addition of defined amounts of water indicate an increase in the reaction order of the amine and a decrease in the reaction order of the enol ether. On the other hand, additional thermal effects become visible by

reaction calorimetry, complicating the analysis. Thus, further studies are needed to unravel the complex kinetic role of water.

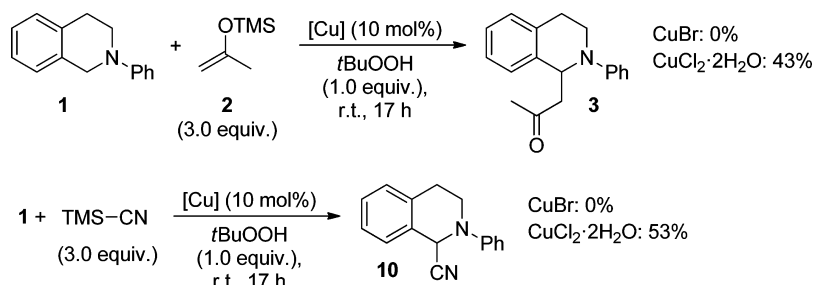
Activating Silyl Nucleophiles in Reactions Using *t*BuOOH as Oxidant. In light of these findings, our previous observation that CuBr completely fails as catalyst in the reaction under study makes sense.⁷ CuBr was shown to be an active catalyst under aerobic conditions using C–H nucleophiles^{4c,13} and was shown to form an iminium tetrabromodicyprate with **1** under oxygen.^{6a} Its failure in the present reaction must therefore be linked to the attack of the nucleophile **2**. Likewise, our observation that the combination of CuBr as catalyst together with *tert*-butyl hydroperoxide as alternative oxidant fails for silyl nucleophiles (**2**, allyl silanes or TMS-CN)^{6b} can be explained. This method has been developed by the Li group and is highly successful for oxidative coupling reactions between amines such as **1** and various nucleophiles, yet silyl nucleophiles were not reported.¹⁴ In contrast, when we employed $\text{CuCl}_2 \cdot 2\text{H}_2\text{O}$ as catalyst in these reactions with *tert*-butyl hydroperoxide as oxidant and **2** and TMS-CN , respectively, as nucleophiles, the products **3** and **10** were formed in significant amounts (Scheme 5).

It appears that CuCl_2 can easily activate silyl nucleophiles, whereas CuBr , only bearing a single and larger halide counterion, cannot, supporting the postulated interaction between nucleophile and catalyst shown in Scheme 4.

Intermolecular Kinetic Isotope Effect. Previously, we measured an intramolecular kinetic isotope effect (KIE) of 4.5 for the reaction between 1-monodeuterated amine, **1-d₁**, and dimethyl malonate.^{6b} This value indicates that C–H bond cleavage is product-determining but not whether it is also rate-determining.¹⁵ The developed technique of using reaction calorimetry for this study allowed us to easily conduct separate kinetic experiments to determine *intermolecular* kinetic isotope effects. The 1-dideuterated amine **1-d₂** was synthesized from tetrahydroisoquinoline **11** in a four-step sequence following reported procedures (Scheme 6a).¹⁶

When **1-d₂** was subjected to standard reaction conditions, the conversion to product **3-d₁** was found to be only slightly slower than that of **1** (Scheme 6b and Figure 6). Dividing the conversion profile of **1** by that of **1-d₂** reveals a ratio of approximately 1.3 over the course of the reaction, which excludes the cleavage of the C–H bond as the rate-determining step. Reversible C–H bond cleavage appears not to take place, as there was no H/D scrambling observed in product **3-d₁**. In the case of a rate-determining nucleophile addition to a deuterated iminium **4-d₁**, an inverse kinetic isotope effect of <1 would be observed. Thus, the low value of 1.3 suggests a β secondary KIE that arises due to hyperconjugation of the C–H/D bonds to the nitrogen atom during a rate-determining SET step.

Scheme 5. CuCl_2 versus CuBr in Oxidative Coupling Reactions of **1 with Silyl Nucleophiles Using *t*BuOOH as Oxidant**



Scheme 6. Synthesis of the 1-Dideuterated Amine **1-d₂** and Application in the Oxidative Coupling with **2**

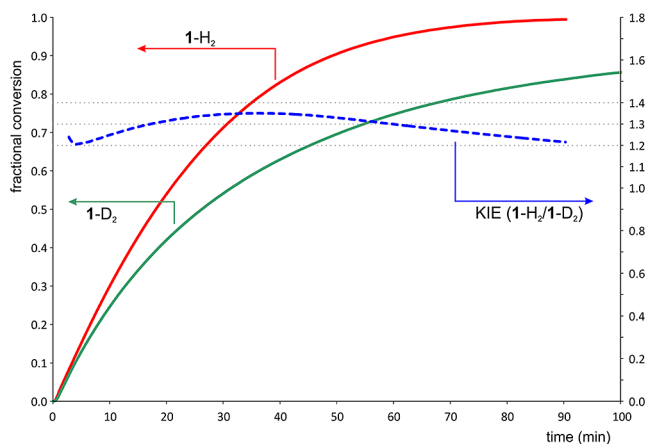
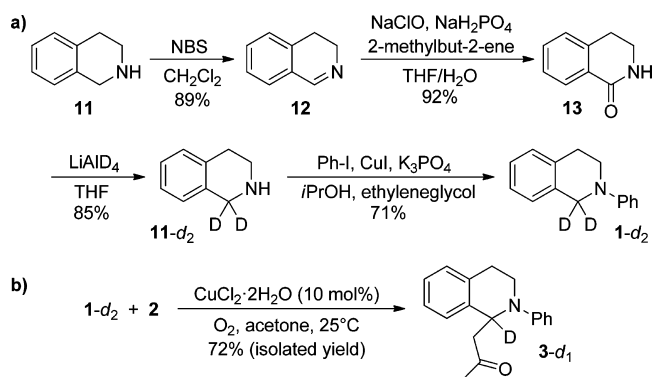


Figure 6. Conversion profiles for reactions with **1** and **1-d₂**, kinetic isotope effect from conversion ratio.

SUMMARY AND CONCLUSIONS

The discussed kinetic experiments provide more details on the mechanism of the aerobic Cu-catalyzed oxidative coupling with *N*-phenyl tetrahydroisoquinoline **1**. The noninteger reaction orders determined for the substrates and the catalyst indicate a complex rate equation, which is approximately half order in amine **1** and 1.25 order in catalyst (eq 2).

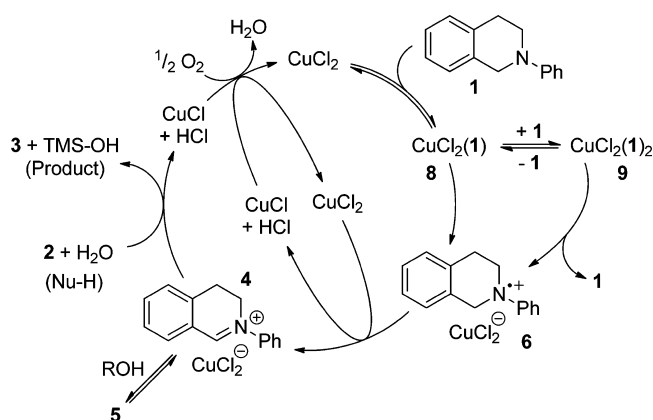
$$r \propto [\mathbf{1}]^{0.45} [\mathbf{2}]^{0.2} [\text{CuCl}_2]^{1.25} \approx [\mathbf{1}]^{0.5} [\text{CuCl}_2]^{1.25} \quad (2)$$

In line with previous mechanistic studies, new conclusions and a refined mechanistic proposal can be derived from these results (Scheme 7).

It is not clear if there is a single rate-controlling step or a combination of steps dominating the reaction rate.¹⁷ In any case, the rate is determined by events preceding C–H bond cleavage and nucleophile addition and therefore is obviously connected to the two single electron transfer steps involved in oxidizing the amine to the iminium ion **4** via radical cation **6**. This hypothesis is supported by the secondary kinetic isotope effect of around 1.3, the positive reaction order in **1**, and the reaction order close to zero found for nucleophile **2**.

These SET reactions could be caused by the coordination of two molecules of amine **1** to the copper catalyst, forming complexes **8** and **9** in equilibrium, as suggested by the reaction order close to 0.5 for this substrate. It is likely that this reduces the precipitation of insoluble species, for example, CuCl(OH), which forms easily from the reduced copper(I) chloride and

Scheme 7. Refined Mechanistic Proposal for the Aerobic Cu-Catalyzed Oxidative Coupling of **1** with **2**



was characterized in reactions at very high catalyst loadings. The higher reaction order of 1.25 in the catalyst supports the involvement of more than one molecule of catalyst in the reaction, which is in line with two separate SET steps, each involving the reduction of Cu(II) to Cu(I). The reoxidation to Cu(II) with oxygen follows the addition of the nucleophile to **4** and is therefore not likely to control the reaction rate.

The computational study by Cheng et al. suggested the first Cu(II)-mediated SET step forming the ammoniumyl radical cation **6** as thermodynamically and kinetically facile, while the subsequent transformation to iminium ion **4** was suggested as rate-determining.^{5b} This involved coordination of Cu(II) to radical cation **6** as the energetically least favored step prior to proton-coupled electron transfer to form **4**, which could also be an explanation for the β secondary KIE.

The fact that the rate actually decreases at very high concentrations of **2** points toward a complex interaction between this substrate and the catalyst. In oxidative coupling reactions of **1** with various silyl nucleophiles, CuCl₂·2H₂O proved to be a superior catalyst to CuBr and CuCl, supporting the role of the chloride counterions in activating the silyl reagents by nucleophilic attack on the silicon atom. Water addition was shown to significantly increase the reaction rate, possibly by accelerating the hydrolysis of the byproduct trimethylsilyl chloride, thereby liberating chloride to regenerate the active catalyst. The role of water is obviously not limited to the formation of the off-cycle hemiaminal **5** shown in Scheme 2a (R = H), which is beneficial for the product yield but does not increase the rate.

EXPERIMENTAL SECTION

General Methods. Unless otherwise indicated, all reagents and solvents were purchased from commercial distributors and used as received. TLC was used to check the reactions for full conversion. TLC spots were visualized by UV-light irradiation and staining with KMnO₄. Flash column chromatography was carried out using silica gel (40–63 μm) with ethyl acetate and pentane of technical grade after distillation in a rotary evaporator. Yields refer to pure isolated compounds. ¹H and ¹³C NMR spectra were measured at 500 and 125 MHz, respectively. All chemical shifts are given in parts per million downfield relative to TMS and were referenced to the solvent residual peaks.¹⁸ ¹H NMR chemical shifts are designated using the following abbreviations as well as their combinations: s = singlet, d = doublet, t = triplet, q = quartet, m = multiplet, br = broad signal. High-resolution mass spectra were recorded with a FTICR-MS, quadrupole MS, and double focusing sector field MS.

Starting Materials. Compounds **1**,^{16d} **13**,^{16b} and **11-d₂**^{16c} were synthesized following reported procedures.

Oxidative Coupling Reactions. Previously reported procedures for the coupling of **1** and **2** using CuCl₂·2H₂O under oxygen⁷ and for the coupling of **1** with nucleophiles using CuBr and *t*BuOOH were followed.^{6b, f4b} Spectroscopic data of the products **3** and **9** were identical with those of previous reports.^{6b, 7}

Kinetic Experiments by Reaction Calorimetry. Into a 10 mL screw-cap vial were placed *N*-phenyl tetrahydroisoquinoline **1**, silyl enol ether **2**, and acetone. The vial was equipped with a magnetic stirring bar, flushed with oxygen, and closed with a pierceable screw cap. The vial was placed into the reactor port of a reaction calorimeter and connected to an external oxygen balloon via a cannula and silicon tube. A syringe filled with a solution of CuCl₂·H₂O in acetone (1.3 wt %) was placed into a temperature-controlled syringe port. Reactions were conducted at 25 °C, and thermal equilibrium was attained after keeping the vials within the calorimeter for at least 25 min and the syringes for at least 15 min. The reactions were initiated by injecting the catalyst solution. The injected amount was determined by subtracting the amount remaining in the syringe from the one filled into it. The reaction progress could be controlled online. Agitation speed was 300 mot/min.

The reaction conversion after completion of the reaction was determined by taking a sample from the reaction mixture by syringe and quenching it by injection into a well-stirred mixture of a saturated aqueous solution of NaHCO₃ and ethyl acetate. After extracting the aqueous phase two more times with ethyl acetate, drying the combined organic phases by passing over MgSO₄, and removing the solvent in vacuum, we redissolved the residue in DMSO-*d*₆ and analyzed it with ¹H NMR spectroscopy. Conversion at the end of the reaction, *f*_{conv}(*t*_{end}), was determined from the ratio of substrate to product peak integrals (**1** vs **3**). A purified sample of **3** was obtained according to a published procedure.⁷ Data points were taken every 6 s over the course of the reaction. The calorimetric experiments were evaluated according to known procedures and techniques.^{10b} The reaction heat flow *q* is proportional to the reaction rate *r*, where Δ*H*_{rxn} is the heat of the reaction and *V* is the reaction volume (eq 3).

$$r = \frac{dq}{dt} = \Delta H_{\text{react}} \times V \times r \quad (3)$$

The observed heat flow profiles may also be used to obtain the fractional conversion *f*_{conv} of the limiting substrate by calculation of the fractional area under the temporal heat flow curve, as given in eq 4, where the numerator represents the area under the heat flow curve at any time point *t* and the denominator represents the total area under the heat flow curve after completion of the reaction at time *t*_{end}.

$$f_{\text{conv}} = f_{\text{conv}}(t_{\text{end}}) \times \frac{\int_0^t q(t) dt}{\int_0^{t_{\text{end}}} q(t) dt} \quad (4)$$

Conversion determined from heat flow was compared to conversion by NMR measurement, determined by taking samples from one reaction over the course of the reaction, quenching, and analyzing them as described above. This confirmed that the observed heat flow represents an accurate measure of rate of the reaction under study.

3,4-Dihydroisoquinoline (12). Synthesis followed a related published procedure.^{16a} *N*-Bromosuccinimide (14.7 g, 82.64 mmol) was added to a methylene chloride solution (113 mL) containing 1,2,3,4-tetrahydroisoquinoline **11** (10 g, 75.12 mmol) under ice-cooling over 20 min. After being stirred for 2 h, an aqueous 30% sodium hydroxide solution (50 mL) was added to the reaction solution. The organic layer was washed with water and then extracted with a 10% aqueous hydrochloric acid solution (50 mL). The aqueous layer was washed with methylene chloride, basified with aqueous ammonia, and then extracted with methylene chloride. The extract was dried over magnesium sulfate and then evaporated. The resulting residue was obtained as a yellow oil with 88.6% (8.72 g) isolated yield and was directly used in the next step without further purification: ¹H NMR (500 MHz, DMSO) δ 8.33 (t, *J* = 2.06 Hz, 1H), 7.41–7.30 (m,

3H), 7.23–7.20 (m, 1H), 3.64 (dt, *J* = 2.16 and 8.85 Hz, 2H), 2.68 (t, *J* = 7.84 Hz, 2H); ¹³C NMR (125 MHz, DMSO) δ 159.5, 136.0, 131.0, 128.2, 127.4, 127.1, 127.0, 46.8, 24.3; HRMS-(EI) (*m/z*) calcd for C₉H₉N⁺ 131.073498, found 131.073368.

2-Phenyl-1,2,3,4-tetrahydroisoquinoline-1,1-[²H₂] (1-d₂). This was prepared by a procedure reported for the nondeuterated compound^{16d} and isolated by column chromatography in 71% yield as a white solid: ¹H NMR (500 MHz, DMSO) δ 7.25–7.13 (m, 6H), 7.01–6.96 (m, 2H), 6.74 (app. t, *J* = 7.15 Hz, 1H), 3.52 (t, *J* = 5.89 Hz, 2H), 2.89 (t, *J* = 5.89 Hz, 2H); ¹³C NMR (125 MHz, DMSO) δ 150.1, 134.7, 134.4, 129.1, 128.4, 126.6, 126.2, 125.9, 117.9, 114.7, 45.6, 28.0; HRMS-(EI) (*m/z*) calcd for C₁₅H₁₃N₁D₂⁺ 211.133001, found 211.133092.

1-(2-Phenyl-1,2,3,4-tetrahydroisoquinolin-1-yl)-1-[²H]-propan-2-one (3-d₁). This was prepared by a procedure reported for the nondeuterated compound⁷ and isolated by column chromatography in 72% yield as a white solid: ¹H NMR (500 MHz, DMSO) δ 7.21–7.11 (m, 6H), 6.97–6.92 (m, 2H), 6.68 (app. t, *J* = 7.25 Hz, 1H), 3.68 (ddd, *J* = 4.1, 5.7, and 13.4 Hz, 1H), 3.50 (ddd, *J* = 4.7, 9.9, and 13.4 Hz, 1H), 3.06 (d, *J* = 16.4 Hz, 1H), 2.93 (ddd, *J* = 5.7, 9.9, and 16.5 Hz, 1H), 2.85 (d, *J* = 16.4 Hz, 1H), 2.74 (app. dt, *J* = 4.3 and 16.4 Hz, 1H), 2.07 (s, 3H); ¹³C NMR (125 MHz, DMSO) δ 206.9, 148.8, 138.1, 134.4, 129.2, 128.7, 126.7, 126.6, 125.9, 117.6, 114.4, 43.5, 40.6, 30.5, 25.6; HRMS (*m/z*) calcd for C₁₈H₁₈N₁O₁D₁Na⁺ [M + Na]⁺ 289.142162, found 289.141903.

■ ASSOCIATED CONTENT

Supporting Information

Complete copies of ¹H and ¹³C NMR spectra for compounds **13**, **11-d₂**, **1-d₂**, and **3-d₁** and additional kinetic experiments. This material is available free of charge via the Internet at <http://pubs.acs.org>.

■ AUTHOR INFORMATION

Corresponding Author

*E-mail: klusi@mpi-muelheim.mpg.de.

Author Contributions

M.S. and A.S. contributed equally.

Notes

The authors declare no competing financial interest.

■ ACKNOWLEDGMENTS

Support from the DFG (Heisenberg scholarship to M.K., KL 2221/4-1), the MPI fuer Kohlenforschung, and Prof. Benjamin List is gratefully acknowledged.

■ REFERENCES

- (1) (a) Girard, S. A.; Knauber, T.; Li, C.-J. *Angew. Chem., Int. Ed.* **2014**, *53*, 74–100. (b) Zheng, C.; You, S.-L. *RSC Adv.* **2014**, *4*, 6173–6214. (c) Jia, F.; Li, Z. *Org. Chem. Front.* **2014**, *1*, 194–214. (d) Zhang, C.; Tang, C.; Jiao, N. *Chem. Soc. Rev.* **2012**, *41*, 3464–3484. (e) Rohlmann, R.; Mancheño, O. G. *Synlett* **2013**, *24*, 6–10. (f) Yeung, C. S.; Dong, V. M. *Chem. Rev.* **2011**, *111*, 1215–1292. (g) Liu, C.; Zhang, H.; Shi, W.; Lei, A. *Chem. Rev.* **2011**, *111*, 1780–1824. (h) Klussmann, M.; Sureshkumar, D. *Synthesis* **2011**, 353–369. (i) Scheuermann, C. J. *Chem.—Asian J.* **2010**, *5*, 436–451. (j) Sun, C.-L.; Li, B.-J.; Shi, Z.-J. *Chem. Commun.* **2010**, 46, 677–685. (k) Sarhan, A. A. O.; Bolm, C. *Chem. Soc. Rev.* **2009**, *38*, 2730–2744. (l) Dick, A. R.; Sanford, M. S. *Tetrahedron* **2006**, *62*, 2439–2463.
- (2) (a) Gulzar, N.; Schweitzer-Chaput, B.; Klussmann, M. *Catal. Sci. Technol.* **2014**, *4*, 2778–2796. (b) Shi, Z.; Zhang, C.; Tang, C.; Jiao, N. *Chem. Soc. Rev.* **2012**, *41*, 3381–3430. (c) Campbell, A. N.; Stahl, S. S. *Acc. Chem. Res.* **2012**, *45*, 851–863. (d) Wendlandt, A. E.; Suess, A. M.; Stahl, S. S. *Angew. Chem., Int. Ed.* **2011**, *50*, 11062–11087.

- (3) (a) Qin, Y.; Lv, J.; Luo, S. *Tetrahedron Lett.* **2014**, *55*, 551–558. (b) Jones, K. M.; Klussmann, M. *Synlett* **2012**, *23*, 159–162. (c) Ravelli, D.; Fagnoni, M. *ChemCatChem* **2012**, *4*, 169–171.
- (4) For examples of metal-catalyzed reactions using oxygen, see: (a) Murata, S.; Miura, M.; Nomura, M. *Chem. Commun.* **1989**, 116–118. (b) Murahashi, S.-I.; Komiya, N.; Terai, H.; Nakae, T. *J. Am. Chem. Soc.* **2003**, *125*, 15312–15313. (c) Baslé, O.; Li, C.-J. *Green Chem.* **2007**, *9*, 1047–1050. (d) Shen, Y.; Tan, Z.; Chen, D.; Feng, X.; Li, M.; Guo, C.-C.; Zhu, C. *Tetrahedron* **2009**, *65*, 158–163. (e) Singhal, S.; Jain, S. L.; Sain, B. *Chem. Commun.* **2009**, 2371–2372. (f) Alagiri, K.; Prabhu, K. R. *Org. Biomol. Chem.* **2012**, *10*, 835–842. (g) Xie, J.; Li, H.; Zhou, J.; Cheng, Y.; Zhu, C. *Angew. Chem., Int. Ed.* **2012**, *51*, 1252–1255.
- (5) (a) Hu, J.; Wang, J.; Nguyen, T. H.; Zheng, N. *Beilstein J. Org. Chem.* **2013**, *9*, 1977–2001. (b) Cheng, G.-J.; Song, L.-J.; Yang, Y.-F.; Zhang, X.; Wiest, O.; Wu, Y.-D. *ChemPlusChem* **2013**, *78*, 943–951. (c) Ratnikov, M. O.; Doyle, M. P. *J. Am. Chem. Soc.* **2013**, *135*, 1549–1557. (d) Yamaguchi, K.; Wang, Y.; Mizuno, N. *ChemCatChem* **2013**, *5*, 2835–2838. (e) Tsang, A. S.-K.; Jensen, P.; Hook, J. M.; Hashmi, A. S. K.; Todd, M. H. *Pure Appl. Chem.* **2011**, *83*, 655–665. (f) Baslé, O.; Borduas, N.; Dubois, P.; Chapuzet, J. M.; Chan, T.-H.; Lessard, J.; Li, C.-J. *Chem.—Eur. J.* **2010**, *16*, 8162–8166. (g) Wang, M.-Z.; Zhou, C.-Y.; Wong, M.-K.; Che, C.-M. *Chem.—Eur. J.* **2010**, *16*, 5723–5735. (h) Murahashi, S.-I.; Naota, T.; Yonemura, K. *J. Am. Chem. Soc.* **1988**, *110*, 8256–8258.
- (6) (a) Boess, E.; Sureshkumar, D.; Sud, A.; Wirtz, C.; Farès, C.; Klussmann, M. *J. Am. Chem. Soc.* **2011**, *133*, 8106–8109. (b) Boess, E.; Schmitz, C.; Klussmann, M. *J. Am. Chem. Soc.* **2012**, *134*, 5317–5325.
- (7) Sureshkumar, D.; Sud, A.; Klussmann, M. *Synlett* **2009**, 1558–1561.
- (8) (a) Murata, S.; Teramoto, K.; Miura, M.; Nomura, M. *Bull. Chem. Soc. Jpn.* **1993**, *66*, 1297–1298. (b) Nishino, M.; Hirano, K.; Satoh, T.; Miura, M. *J. Org. Chem.* **2011**, *76*, 6447–6451. (c) Tanoue, A.; Yoo, W.-J.; Kobayashi, S. *Adv. Synth. Catal.* **2013**, *355*, 269–273.
- (9) Nelsen, S. F.; Ippoliti, J. T. *J. Am. Chem. Soc.* **1986**, *108*, 4879–4881.
- (10) (a) Blackmond, D. G. *Angew. Chem., Int. Ed.* **2005**, *44*, 4302–4320. (b) Mathew, J. S.; Klussmann, M.; Iwamura, H.; Valera, F.; Futran, A.; Emanuelsson, E. A. C.; Blackmond, D. G. *J. Org. Chem.* **2006**, *71*, 4711–4722. (c) Zotova, N.; Valera, F.; Blackmond, D. G. *Chem. Ind.* **2009**, 123, 445–454.
- (11) (a) LeBlond, C.; Wang, J.; Larsen, R. D.; Orella, C. J.; Forman, A. L.; Landau, R. N.; Laquidara, J.; Sowa, J. R.; Blackmond, D. G.; Sun, Y. K. *Thermochim. Acta* **1996**, *289*, 189–207. (b) Ferretti, A. C.; Mathew, J. S.; Blackmond, D. G. *Ind. Eng. Chem. Res.* **2007**, *46*, 8584–8589.
- (12) (a) El-Sayed, M. A.; Salam, A. H. A.; Abo-El-Dahab, H. A.; Refaat, H. M.; El-Dissouky, A. L. I. *J. Coord. Chem.* **2009**, *62*, 1015–1024. (b) El-Sayed, M. A.; El-Toukhy, A.; Davies, G. *Inorg. Chem.* **1985**, *24*, 3387–3390.
- (13) Baslé, O.; Li, C.-J. *Chem. Commun.* **2009**, 4124–4126.
- (14) (a) Li, Z.; Li, C.-J. *J. Am. Chem. Soc.* **2004**, *126*, 11810–11811. (b) Li, Z.; Bohle, D. S.; Li, C.-J. *Proc. Natl. Acad. Sci. U.S.A.* **2006**, *103*, 8928–8933. (c) Zhao, L.; Li, C.-J. *Angew. Chem., Int. Ed.* **2008**, *47*, 7075–7078.
- (15) Simmons, E. M.; Hartwig, J. F. *Angew. Chem., Int. Ed.* **2012**, *51*, 3066–3072.
- (16) (a) Toshiaki, W.; Yasuhiro, F.; Naoko, H.; Taro, S.; Yuji, Y.; Toru, H.; Takashi, O.; Akihiko, T.; Junichi, K.; Tadashi, O.; Keiko, T.; Kazumasa, N.; Shinichi, H.; Norihiro, U. Integrin expression inhibitors. U.S. Patent EP1258252 (A1), 2002. (b) Mohamed, M. A.; Yamada, K.-i.; Tomioka, K. *Tetrahedron Lett.* **2009**, *50*, 3436–3438. (c) Chen, L.; Zhang, L.; Lv, J.; Cheng, J.-P.; Luo, S. *Chem.—Eur. J.* **2012**, *18*, 8891–8895. (d) Li, Z.; Li, C.-J. *J. Am. Chem. Soc.* **2005**, *127*, 6968–6969.
- (17) For a discussion of the concept of rate-controlling steps, see: Laidler, K. J. *J. Chem. Educ.* **1988**, *65*, 250.
- (18) Gottlieb, H. E.; Kotlyar, V.; Nudelman, A. *J. Org. Chem.* **1997**, *62*, 7512–7515.